SUPPLEMENTARY FIGURE 1

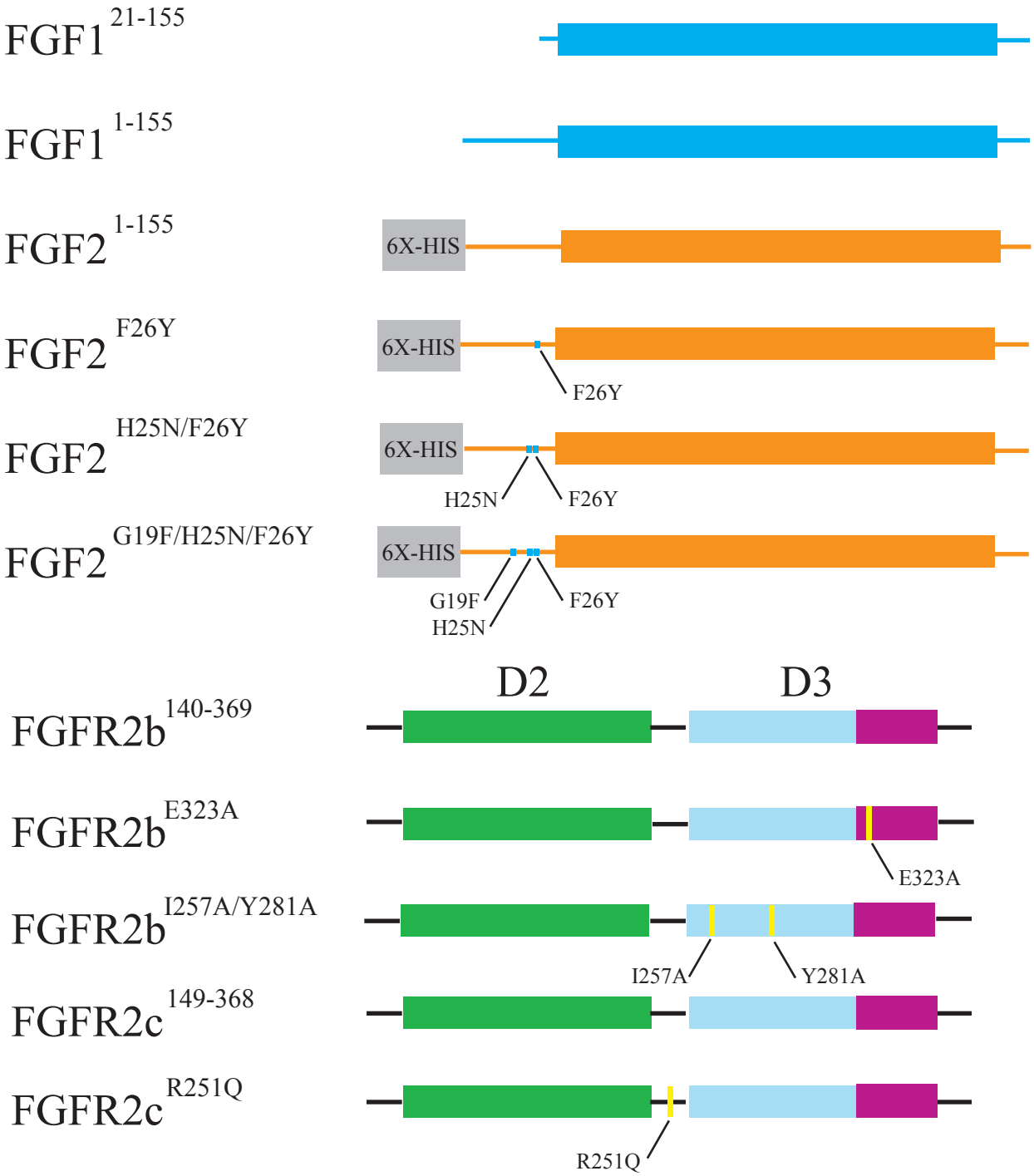

SUPPLEMENTARY FIGURE 2

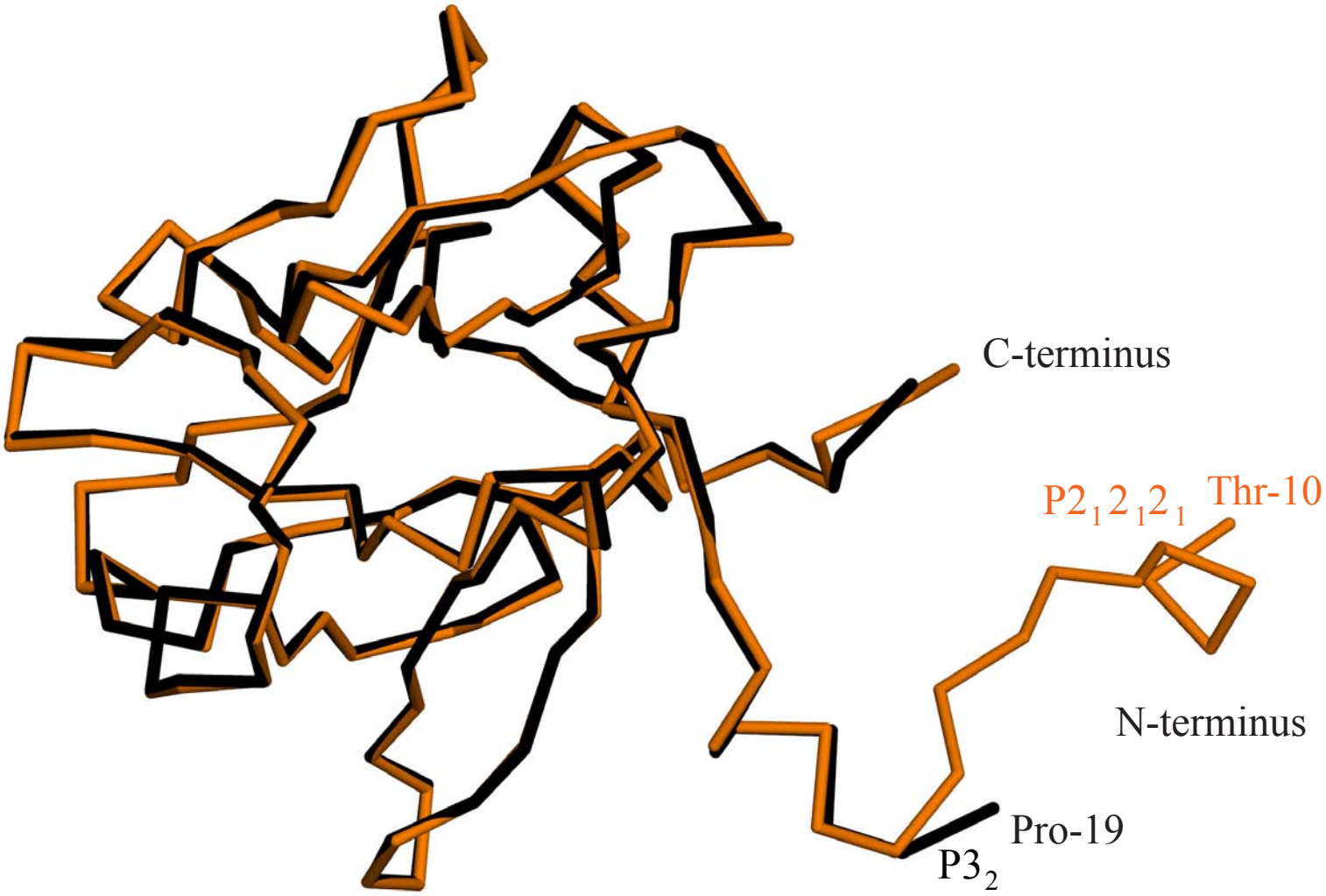

SUPPLEMENTARY FIGURE 3

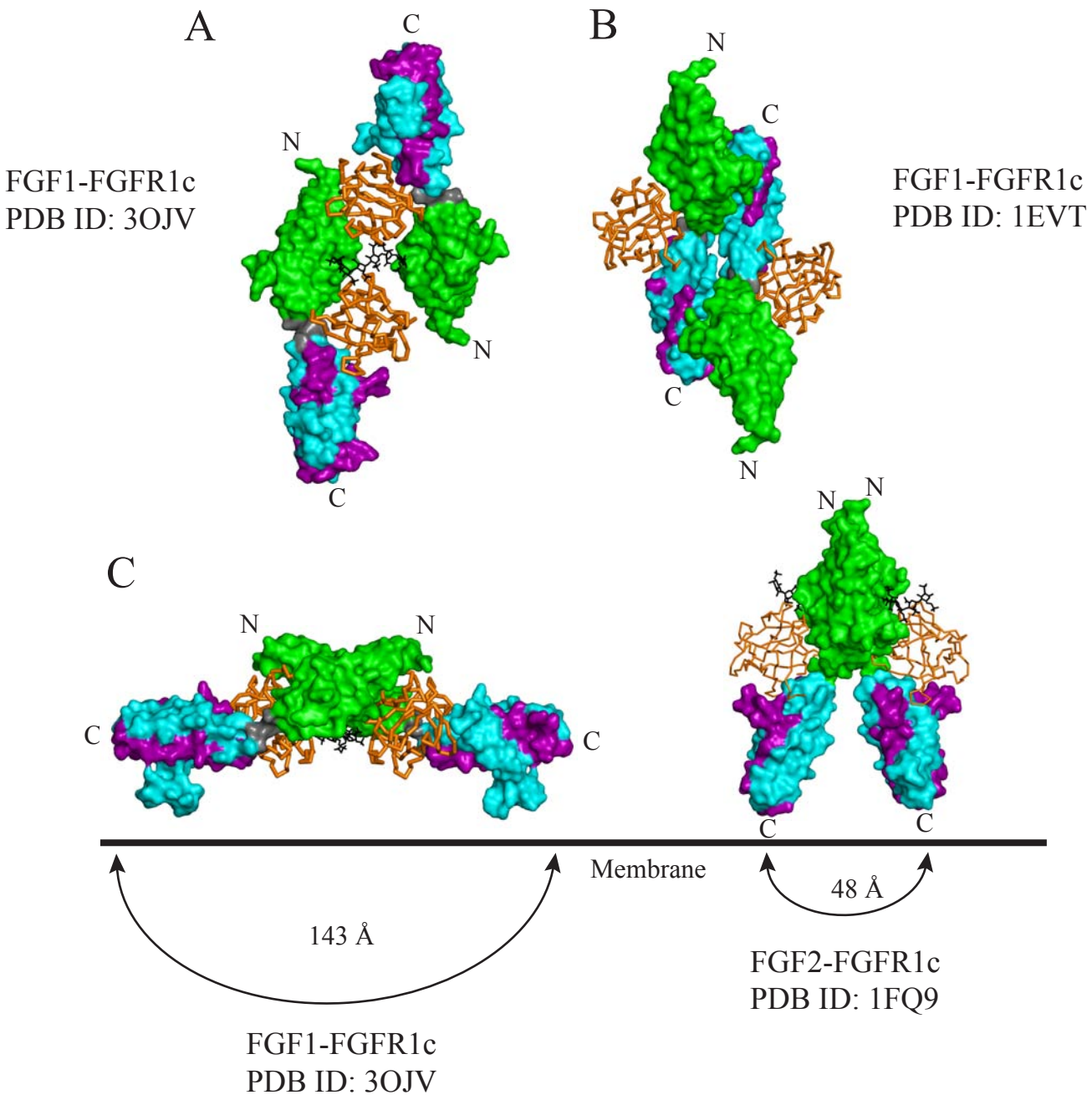

SUPPLEMENTARY FIGURE 4

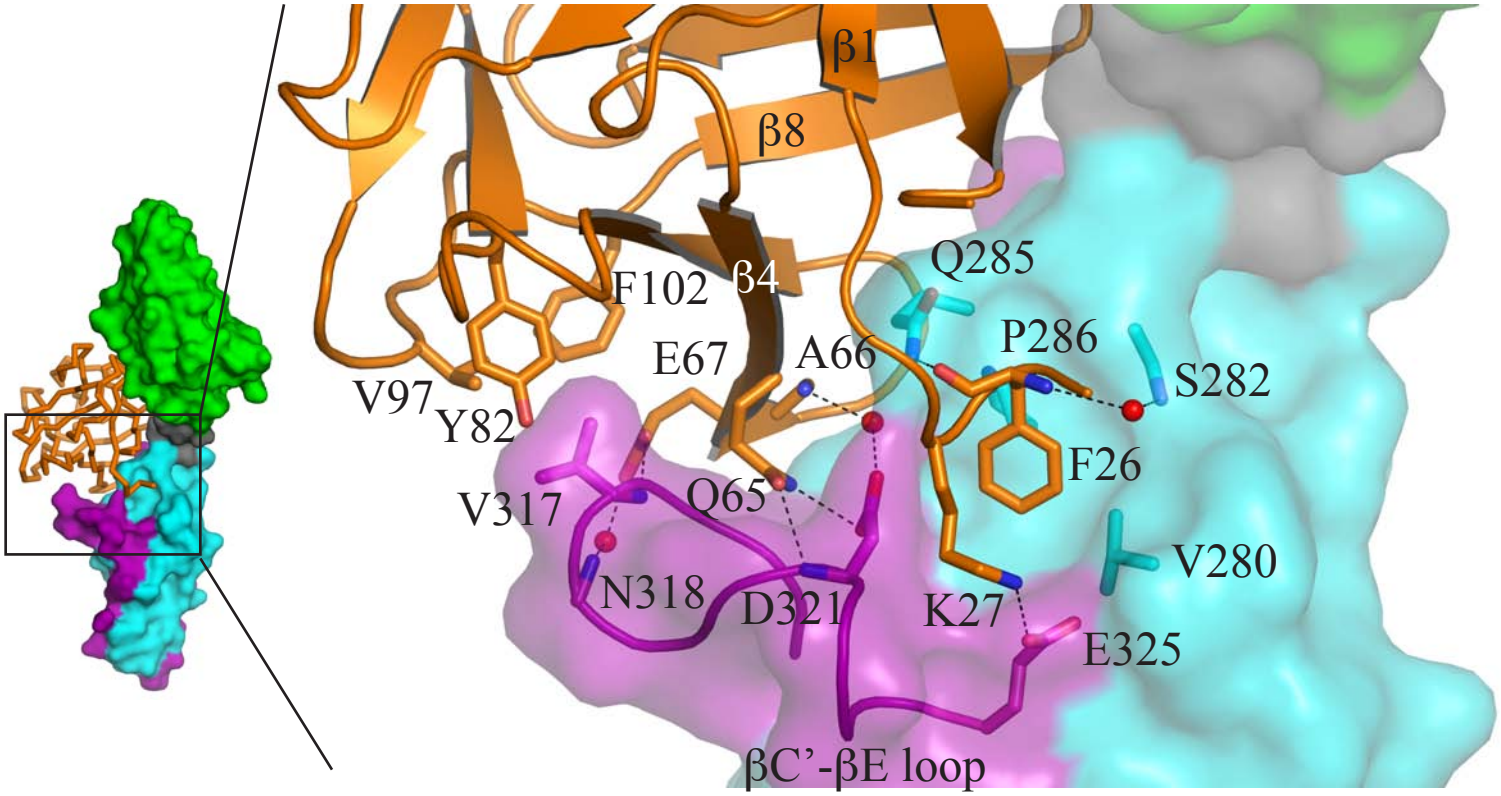

FGF2-FGFR2c
(PDB ID: 1EV2)

SUPPLEMENTARY FIGURE 5

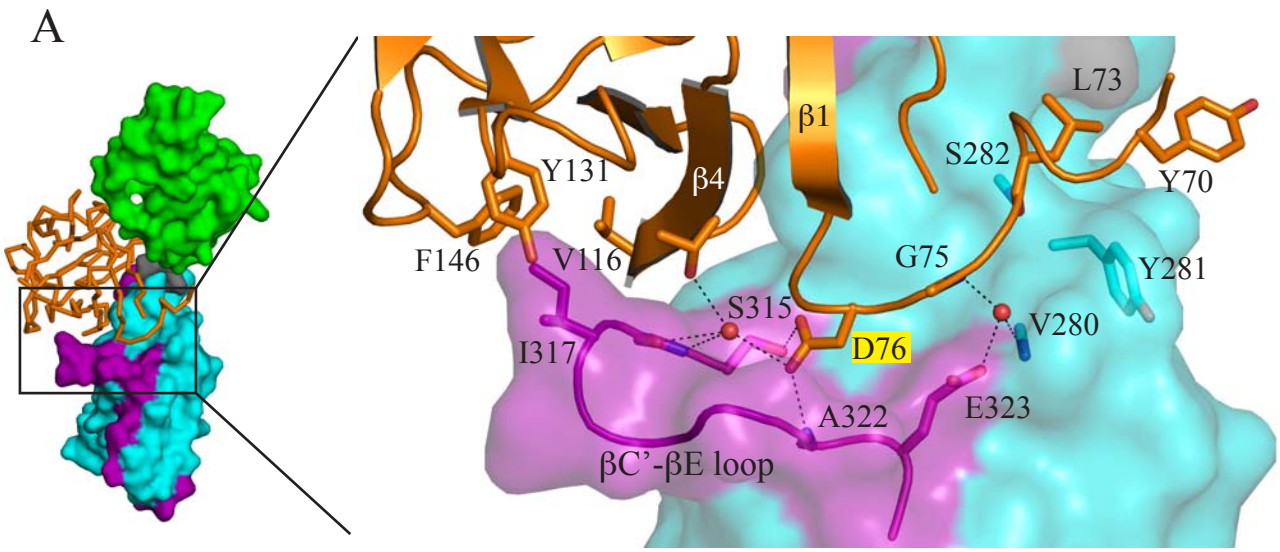

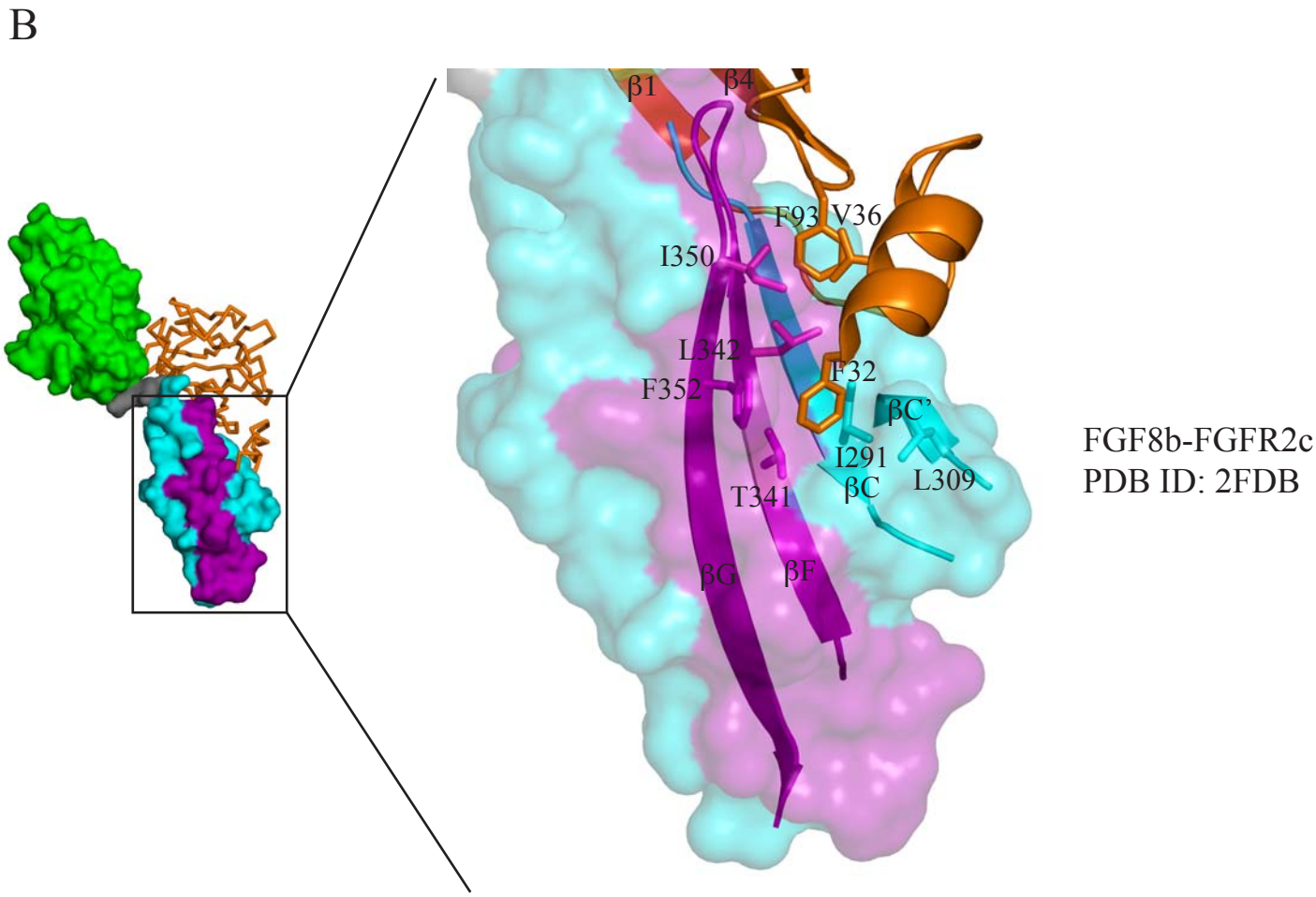

SUPPLEMENTARY FIGURE 6

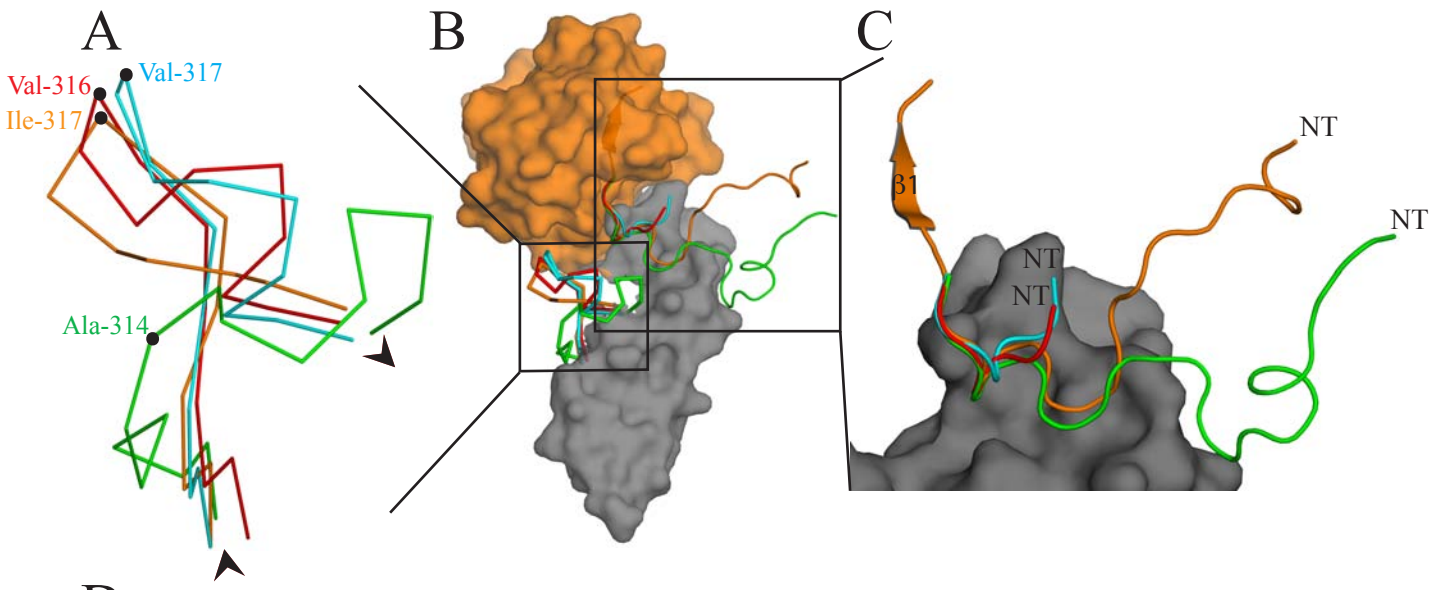

D

```
                  βA                  βA'                 βB                  βB'                 βC                  βC'                 βD
FGFR2b (153) APYWTNTEKM  EKRLHAVPAA  NTVKFRCPAG  GNPMPTMRWL  KNGKEFKQEH  RIGGYKVRNQ (212)
FGFR2c (153) ..........  ..........  ..........  ..........  ..........  ..........  .......... (212)
FGFR1b (152) .....SP...  ..K.......  K....K..SS  .T.N..L...  ........PD.  .........YA (211)
FGFR1c (152) .....SP...  ..K.......  K....K..SS  .T.N..L...  ........PD.  .........YA (211)
FGFR3b (150) .....RP.R.  D.K.L.....  ...R.....A  ...T.SIS..  ...R..RG..  ....I.L.H. (209)
FGFR3c (150) .....RP.R.  D.K.L.....  ...R.....A  ...T.SIS..  ...R..RG..  ....I.L.H. (209)
FGFR4  (146) .....HPQR.  ..K......G  ..........A  ...T..I...  .D.QA.HG.N  ....IRL.H. (205)

                  βE                  βF                  βG                  βA                  βA'
FGFR2b (213) HWSLIMESVV  PSDKGNYTCV  VENEYGSINH  TYHLDVVERS  PHRPILQAGL  PANASTVVGG (272)
FGFR2c (213) ..........  ..........  ..........  ......E...  ..........  .......... (272)
FGFR1b (212) T..I..D...  ..........  ..........  ..Q.......  ..........  ...KTVAL.S (271)
FGFR1c (212) T..I..D...  ..........  ..........  ..Q.....E.  ..........  ...KTVAL.S (271)
FGFR3b (210) Q...V.....  ...R......  ...KF...RQ  ..T...L...  ..........  ...QTA.L.S (269)
FGFR3c (210) Q...V.....  ...R......  ...KF...RQ  ..T...L...  ..........  ...QTA.L.S (269)
FGFR4  (206) ....V.....  ...R.T...L  ...AV...RY  N.L...L...  ..........  ...TTA...S (265)

                  βB   βB'            βC                  βC'                 βE
FGFR2b (273) DVEFVCKVYS  DAQPHIQWIK  HVEKNGSKYG  PDGLPYLKVL  KHSGINSSN-  -AEVLALFNV (330)
FGFR2c (273) .......E..  ..E.......  ..........  ..........  .AA.V.TTDK  EI...YIR.. (332)
FGFR1b (272) N...M.....  .P.......L.  .I.V....I.  ...N...VQI.  .........D  -....T.... (329)
FGFR1c (272) N...M.....  .P.......L.  .I.V....I.  ...N...VQI.  .TA.V.TTDK  EM...H.R.. (331)
FGFR3b (270) ....H.....  ..........L.  ...V....V.  ...T..VT..  .SWISE.VE-  ADVR.R.A.. (328)
FGFR3c (270) ....H.....  ..........L.  ...V....V.  ...T..VT..  .TA.A.TTDK  EL...S.H.. (329)
FGFR4  (266) ...LL.....  ..........L.  .IVI...SF.  A..F..VQ..  .TAD....E-  -V...Y.R.. (323)

                  βF                  βG
FGFR2b (331) TEADAGEYIC  KVSNYIGQAN  QSAWLTVL (358)
FGFR2c (333) .FE.....T.  LAG.S..ISF  H....... (360)
FGFR1b (330) ...QS...V.  ..........  .......T (357)
FGFR1c (332) SFE.....T.  LAG.S..LSH  H....... (359)
FGFR3b (329) S.R.G...L.  RAT.F..V.E  KAF..S.H (356)
FGFR3c (330) .FE.....T.  LAG.S..FSH  H....V.. (357)
FGFR4  (324) SAE.....T.  LAG.S..LSY  ........ (351)
```

βC'-βE Loop

SUPPLEMENTARY FIGURE 7

A

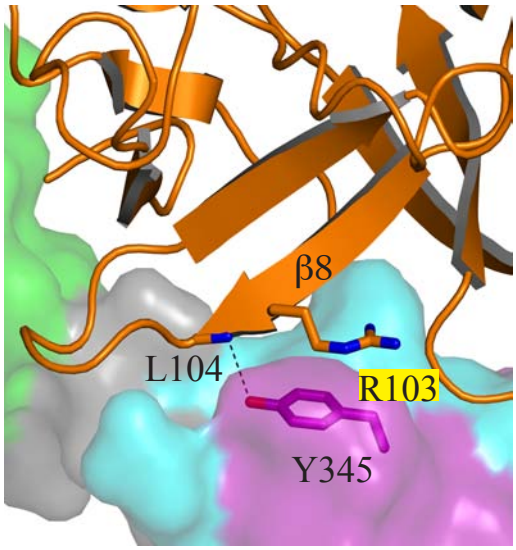

FGF1-FGFR2b
PDB ID: 3OJM

B

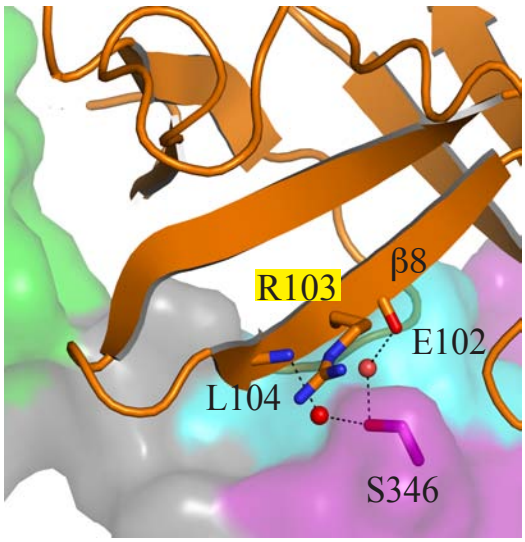

FGF1-FGFR1c
PDB ID: 3OJV

C

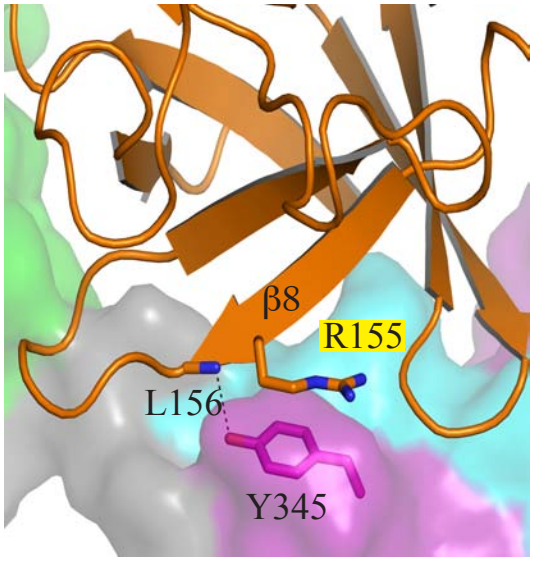

FGF10-FGFR2b
PDB ID: 1NUN

D

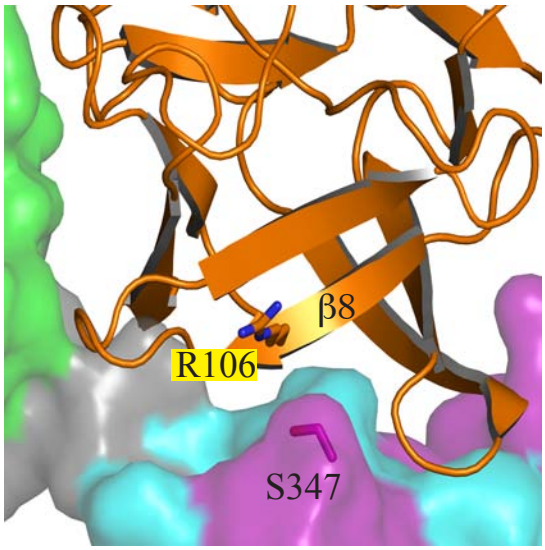

FGF2-FGFR2c
PDB ID: 1EV2

Supplementary Figure 1. Schematic of wild-type and mutated FGF and FGFR proteins used in this study. The β-trefoil core domain of FGFs and the Ig-like domains of FGFRs are represented as boxes. The hexahistidine- tag at the N-terminus of the FGF2 constructs is indicated by a grey box. FGF1 and FGF2 proteins are colored in cyan and orange, respectively. For the FGFRs, the D2 domain is colored in green, the common portion of the D3 domain is colored in light blue, and the spliced portion of the D3 domain is colored in purple. In the mutated FGF2 constructs, the positions of the mutations that were introduced into FGF2 to convert FGF2 into FGF1 are indicated by small cyan boxes and the notations for the mutations are given. The locations of the mutations that were introduced into FGFR2b and FGFR2c are indicated by yellow bars, and the notation for the mutations is given.

Supplementary Figure 2. The N-terminus of FGF1 is more ordered in the FGF1-FGFR2b^{P253R} ($P2_12_12_1$) structure than in the FGF1-FGFR2b^{A172F} ($P3_2$) structure. Shown is a superimposition of the Cα traces of FGF1 from the $P2_12_12_1$ (orange) and $P3_2$ (black) crystal forms of the FGF1-FGFR2b complex. The RMS deviation for the superimposition of the Cα traces of residues 20 through 151 of FGF1 in these two structures is only 0.3Å. The additional ordering of residues Thr-10 to Leu-18 at the N-terminus of FGF1 in the FGF1-FGFR2b^{P253R} structure is attributable to contacts of these residues with the D2 domain of FGFR2b.

Supplementary Figure 3. Differences in the crystal lattice contacts between the new FGF1-FGFR1c-octasaccharide structure (PDB ID: 3OJV) and the first FGF1-FGFR1c structure (PDB ID: 1EVT) give rise to differing assemblies of the two FGF-FGFR complexes in the asymmetric units of these two structures. The molecular surfaces of the receptors and the Cα traces of the ligands are shown. Note that there are no contacts between the receptors in 3OJV (panel A), whereas in 1EVT (panel B) the two receptors engage each other extensively. Only six sugar rings of the octasaccharide (shown as black sticks) are ordered in 3OJV. The oligosaccharide is sandwiched between the heparin binding sites of the two FGF1 ligands, but it does not interact with the heparin binding site on the D2 domain of either receptor. As shown in panel C, the two FGF1-FGFR1c complexes in 3OJV are anti-parallel and nearly co-planar to each other, such that the C-terminal membrane insertion points of the D3 domains of the receptors are 143 Å apart and point in opposite directions. Hence, the mode of receptor dimerization by the heparin octasaccharide in 3OJV (panel A) is non-physiological. For comparison, the crystal structure of the 2:2:2 FGF2-FGFR1c-heparin symmetric dimer (PDB ID: 1FQ9) is shown in panel C. "N" and "C' denote the N- and C-termini of the receptors.

Supplementary Figure 4. The contacts between FGF2 and the βC'-βE loop of FGFR2c as observed in the FGF2-FGFR2c structure (PDB ID: 1EV2). Please note that FGF2 makes identical contacts with the βC'-βE loop of FGFR1c in the FGF2-FGFR1c structure (PDB ID: 1CVS). The hydrogen bonds between Gln-65 of FGF2 and Asp-321 in the βC'-βE loop of receptor restrict the receptor binding specificity of FGF2 to only 'c' isoforms of FGFR1 and FGFR2. Glu-67 and Tyr-82 of FGF2 correspond to Glu-64 and Tyr-79 of FGF1 that engage in plastic interactions with FGFRs, suggesting that plasticity in the interaction of these two residues of FGF1 with FGFRs does not contribute to FGF1's promiscuity. In the close-up view of the structure, the receptor and the ligand are shown as a molecular surface and ribbon, respectively.

Supplementary Figure 5. The N-termini of FGF10 and FGF8b dictate the specificity of these ligands for their cognate FGFRs. (A) Selected contacts at the FGF-D3 interface of the FGF10-FGFR2b structure (PDB ID: 1NUN). FGF10's specificity for FGFR2b can be accounted for by the specific hydrogen bonding between Asp-76 of FGF10 and Ser-315 in the βC'-βE loop of FGFR2b. Note that Asp-76 (highlighted in yellow) occupies the same position as Tyr-23 in FGF1, a residue that plays a key role in FGF1's promiscuity. (B) The binding specificity of FGF8b for FGFR1c-FGFR3c and FGFR4 can be traced to hydrophobic contacts between Phe-32 and Val-36 of the FGF8b N-terminus and Phe-93 of the FGF8b β4–β5 loop and a conserved hydrophobic groove in D3 of FGFR1-FGFR3c and FGFR4. In the

close-up view of the structures, the receptor and the ligand are shown as a molecular surface and ribbon, respectively.

Supplementary Figure 6. The conformation of the βC'-βE loop in D3 differs in each FGF1-FGFR structure and is dictated by contacts with FGF1. (A) Comparison of βC'-βE loop conformations from the four different FGF1-FGFR structures. For the purpose of comparison, the four complexes were superimposed by means of aligning the core region of FGF1. FGFR2b is in orange (PDB ID: 3OJM), FGFR1c is in red (PDB ID: 3OJV), FGFR2c is in cyan (PDB ID: 1DJS), and FGFR3c is in green (PDB ID: 1RY7). The residues from the βC'-βE loops of FGFR1c, FGFR2c, and FGFR2b that engage in hydrophobic contacts with core residues of FGF1 are labeled. Note that Ala-314 of FGFR3c cannot make strong hydrophobic contacts with the core region of FGF1 and as the result the entire βC'-βE loop falls away from the FGF1 core. (B) The FGF1-FGFR2b complex (PDB ID: 3OJM) with ligand depicted as an orange surface and D3 of receptor as a grey surface. For the sake of simplicity, D2 of receptor is not shown. The surface of the βC'-βE loop in D3 is removed so that the different conformations of the βC'-βE loop are seen. (C) Comparison of FGF1 N-termini in different FGF1-FGFR structures. In panels B and C, the N-terminus of FGF1 is colored to match the color of its respective bound receptor. N-terminus of FGF1 is denoted by NT, and the β1 strand of FGF1 in FGF1-FGFR2b is shown. (D) Sequence alignment of the seven principal human FGFRs. Red bars above the sequence indicate the locations of β strands in FGFR2b. Residues colored orange participate in direct hydrogen bonds with FGF1 ligand, those colored cyan participate in water-mediated hydrogen bonds, and those colored brown make hydrophobic contacts. Yellow indicates a π-cation interaction. Residues participating in more than one type of interaction have multiple colors. The common portion of the D3 domain is boxed in cyan, and the alternatively spliced portion of the D3 domain is boxed in purple. A black dot indicates the location of residues in the βC'-βE loop of FGFR that make hydrophobic contacts with core residues of FGF1. The location of the βC'-βE loop of receptor is indicated by a shaded grey bar.

Supplementary Figure 7. Plasticity at the interface between FGF1 and the alternatively spliced βF-βG loop of receptor cannot account for FGF1's promiscuity. Panels A and B show side-by-side comparison of the interactions of the β8 strand of FGF1 with the alternatively spliced βF-βG loop of receptor in the FGF1-FGFR2b (PDB ID: 3OJM) and FGF1-FGFR1c (PDB ID: 3OJV) structures. Note that FGFR1c has a Ser-346 at the analogous position to Tyr-345 of FGFR2b. In FGF1-FGFR2b (panel A), Arg-103 of FGF1 makes a π-cation interaction with Tyr-345 in the βF-βG loop of receptor. In contrast, Arg-103 of FGF1 does not participate in receptor binding in the FGF1-FGFR1c structure (PDB ID: 3OJV) (panel B). Instead, in the FGF1-FGFR1c structure (panel B), backbone atoms of the β8 strand of FGF1 are observed to engage Ser-346 of FGFR1c via water-mediated hydrogen bonds. Panel C shows that Arg-155 of FGF10 in the FGF10-FGFR2b structure (PDB ID: 1NUN) makes a π-cation interaction with Tyr-345 in the βF-βG loop of receptor reminiscent of that seen in the FGF1-FGFR2b structure (panel A). Given the fact that FGF10 is a highly specific ligand for FGFR2b, this π-cation interaction is unlikely to contribute to FGF1's promiscuity. (D) The interface between the β8 strand of FGF2 and the alternatively spliced βF-βG loop of receptor in the FGF1-FGFR2c structure (PDB ID: 1EV2). Note that Arg-103 of FGF1 is conserved in FGF2 (Arg-106) suggesting that in principle, Arg-106 of FGF2 could also engage in a π-cation interaction with Tyr-345 in the βF-βG loop of FGFR2b. Since FGF2 binds specifically to FGFR1c and FGFR2c and not FGFR2b, this structural observation implies that plasticity at the interface between β8 strand of FGF1 and the alternatively spliced βF-βG loop is not a key factor in FGF1's promiscuity. The arginines in each structure are highlighted with a yellow box for emphasis. In each panel, the receptor and the ligand are shown as a molecular surface and ribbon, respectively.